University of Nebraska - Lincoln

DigitalCommons@University of Nebraska - Lincoln

Uniformed Services University of the Health Sciences

U.S. Department of Defense

2002

The *Saccharomyces cerevisiae YBR159w* Gene Encodes the 3-Ketoreductase of the Microsomal Fatty Acid Elongase

Gongshe Han
Uniformed Services University of the Health Sciences

Ken Gable
Uniformed Services University of the Health Sciences

Sepp D. Kohlwein
University Graz

Frédéric Beaudoin
Institute of Arable Crops-Long Ashton Research Station

Johnathan A. Napier
Institute of Arable Crops-Long Ashton Research Station

See next page for additional authors

Follow this and additional works at: https://digitalcommons.unl.edu/usuhs

Part of the Medicine and Health Sciences Commons

Authors

Gongshe Han, Ken Gable, Sepp D. Kohlwein, Frédéric Beaudoin, Johnathan A. Napier, and Teresa M. Dunn

The *Saccharomyces cerevisiae YBR159w* Gene Encodes the 3-Ketoreductase of the Microsomal Fatty Acid Elongase*

Gongshe Han‡, Ken Gable‡, Sepp D. Kohlwein§, Frédéric Beaudoin¶, Johnathan A. Napier¶, and Teresa M. Dunn‡||

From the ‡Department of Biochemistry and Molecular Biology, Uniformed Services University of the Health Sciences, Bethesda, Maryland 20184, ¶Institute of Arable Crops-Long Ashton Research Station, Long Ashton, Bristol BS41 9AF, United Kingdom, and the §Department of Molecular Biology, Biochemistry, and Microbiology, SFB Biomembrane Research Center, University Graz, 1 Schubertstrasse, A8010 Graz, Austria

The *YBR159w* gene encodes the major 3-ketoreductase activity of the elongase system of enzymes required for very long-chain fatty acid (VLCFA) synthesis. Mutants lacking the *YBR159w* gene display many of the phenotypes that have previously been described for mutants with defects in fatty acid elongation. These phenotypes include reduced VLCFA synthesis, accumulation of high levels of dihydrosphingosine and phytosphingosine, and accumulation of medium-chain ceramides. *In vitro* elongation assays confirm that the *ybr159∆* mutant is deficient in the reduction of the 3-ketoacyl intermediates of fatty acid elongation. The *ybr159∆* mutant also displays reduced dehydration of the 3-OH acyl intermediates of fatty acid elongation, suggesting that Ybr159p is required for the stability or function of the dehydratase activity of the elongase system. Green fluorescent protein-tagged Ybr159p co-localizes and co-immunoprecipitates with other elongating enzymes, Elo3p and Tsc13p. Whereas VLCFA synthesis is essential for viability, the *ybr159∆* mutant cells are viable (albeit very slowly growing) and do synthesize some VLCFA. This suggested that a functional ortholog of Ybr159p exists that is responsible for the residual 3-ketoreductase activity. By disrupting the orthologs of *Ybr159w* in the *ybr159∆* mutant we found that the *ybr159∆ayr1∆* double mutant was inviable, suggesting that Ayr1p is responsible for the residual 3-ketoreductase activity.

The distinct fatty acid compositions of different cellular membranes highlight the importance of lipid structure and composition for membrane function. The fatty acids are not only structural components of membranes; they are also bioactive metabolites that regulate various cellular processes. Cytosolic fatty acid synthase catalyzes the *de novo* synthesis of the majority of cellular fatty acids, which have 16 or 18 carbons. In contrast, the membrane-associated fatty acid chain-elongating systems synthesize the very long-chain fatty acids (VLCFAs[1]; >18 carbons). The VLCFAs confer unique physical properties upon the lipids into which they are incorporated. Furthermore, different tissues contain structurally distinct VLCFAs, suggesting that they confer tissue-specific functions. For example, the VLCFAs in brain are predominantly saturated or monounsaturated with chain lengths of 24 or 26 carbons; those in the stomach, kidney, and brain are α-hydroxylated; and those in testes, epidermis, and retina are polyunsaturated with chain lengths of up to 34 carbons.

Fatty acid elongation, beyond C16/C18 carbon atoms synthesized by fatty acid synthase in conjunction with Elo1p, is catalyzed by the microsomal "elongase" that consists of four distinct enzymatic reactions. In sequential order, these are a condensation reaction between a CoA-esterified fatty acyl substrate and malonyl-CoA, a 3-ketoacyl-CoA reduction, a 3-hydroxyacyl-CoA dehydration, and a final enoyl-CoA reduction (Fig. 1). Early biochemical studies suggested that the enzymatic activities reside in distinct proteins but that they may associate into a complex that catalyzes fatty acid elongation. In fact, the evidence suggests that there are multiple complexes that elongate different FA substrates. For example, inhibition studies indicated that different proteins are responsible for the elongation of unsaturated and saturated fatty acids and for the elongation of fatty acids of different chain lengths (1). The genetic studies in yeast support these findings, since Elo2p and Elo3p are homologous proteins believed to catalyze the same reaction but with preferences for substrates of different chain lengths.

It has been hypothesized that the specificity of each elongation reaction is conferred through the selectivity of the first and rate-limiting step, the condensation reaction. Investigators working with *Arabidopsis* found that the *FAE1* gene is required for VLCFA synthesis (2–6). The *FAE1* gene was predicted to encode a condensing enzyme (3-ketoacyl-CoA synthase) based on sequence homology with other condensing enzymes (2). Biochemical characterization of the *FAE1* gene from both *Arabidopsis* and jojoba (7) supports the conclusion that Fae1p is involved in VLCFA synthesis. Surprisingly, there is no gene in *Saccharomyces cerevisiae* with significant homology to *FAE1*. On the other hand, the ELO homologs comprise a gene family conserved from yeast to humans that are candidates for a novel class of condensing enzymes. Two lines of experiments identified the *S. cerevisiae ELO2* and *ELO3* genes as being required for VLCFA synthesis. Based on their homol-

---

---

[1] The abbreviations used are: VLCFAs, very long-chain fatty acids; LCB, long-chain base; ER, endoplasmic reticulum; FAMES, fatty acid methyl esters; GCMS, gas chromatography mass spectrometry; SPT, serine palmitoyltransferase; IPC, inositolphosphoceramide; PHS, phytosphingosine; HA, hemagglutinin; GFP, green fluorescent protein.

ogy to *ELO1*, a gene encoding a protein required to convert myristate to palmitate (8, 9), the *ELO2* and *ELO3* genes were determined to be required for VLCFA synthesis (10). We identified a role for the *ELO2* and *ELO3* genes in VLCFA synthesis through the analysis of sphingolipid synthesis mutants (discussed below). Elo2p is involved in elongation of fatty acids up to C22 or C24, whereas Elo3p has a broader substrate specificity and is essential for conversion of C24 to C26 (10).

The hypothesis that the specificity of elongation is conferred by the condensing enzymes is further supported by the observation that heterologous expression in yeast of the plant Fae1p condensing enzyme confers the ability to elongate C18:1 to C20:1 and C22:1, although yeast does not normally elongate monounsaturated fatty acids longer than C16 or C18 fatty acids (11). Similarly, heterologous expression of the *Caenorhabditis elegans* ELO-like PEA1 gene in yeast confers the ability to elongate exogenously supplied polyunsaturated C18 fatty acids, although yeast has only very limited endogenous capacity for synthesizing or elongating polyunsaturated fatty acids (12, 13). We have previously shown that mutants defective in the only yeast fatty acid desaturase, Ole1p, survive if supplemented with unsaturated C14:1Δ9 fatty acids that become elongated to C16:1Δ11 by the Elo1p gene product (14).

In contrast to the Elo enzymes, which are believed to display substrate specificity, it may be that the other elongating enzymes (two reductases and a dehydratase; see Fig. 1) are common components of the microsomal fatty acyl elongases that function to lengthen all of the fatty acid elongase substrates. We recently identified the *TSC13* gene in a screen for temperature-sensitive (ts) mutants with defects in sphingolipid synthesis (15–17) and provided evidence that the *TSC13* gene encodes the enoyl reductase component of the microsomal elongase. Tsc13p was shown to coimmunoprecipitate with the presumptive condensing enzymes, Elo2p and Elo3p. Interestingly, a growth state-dependent enrichment of Tsc13p to sites of vacuole-nuclear envelope interaction was observed, but the significance of this is unclear, and Elo2p and Elo3p do not display this localization. *TSC13* is essential, as is expected for a gene encoding a nonredundant fatty acid-elongating activity.

In recent studies aimed at identifying other enzymatic components of the fatty acid elongase, we found that the *YBR159w* gene is required for reconstituting heterologous (Fae1p- or Pea1p-mediated) elongase activity in yeast. Here we report analysis of the mutants lacking Ybr159p and demonstrate that these mutant cells have many of the phenotypes that we have previously described for the *elo2Δ*, *elo3Δ*, and *tsc13-1* (elongase-defective) mutant cells. These phenotypes indicate that Ybr159p is the major 3-ketoreductase activity required for endogenous VLCFA synthesis in yeast. We report that Ybr159p is a nuclear/endoplasmic reticulum (ER)-localized protein that associates in complexes with Elo3p and Tsc13p. Mutants that are devoid of elongase activity (the *elo2Δelo3Δ* double mutant or the *tsc13Δ* mutant) are inviable, indicating that the VLCFAs are essential. Although it grows poorly, the *ybr159Δ* mutant is viable, indicating that there is another gene that encodes a 3-ketoreductase activity that can function in fatty acid elongation. We provide evidence that the *AYR1* gene, previously reported to encode 1-acyldihydroxyacetone-phosphate reductase activity (18), is responsible for the residual fatty acid elongation activity.

EXPERIMENTAL PROCEDURES

Media, Strains, and Genetic Manipulations—Yeast media were prepared, and cells were grown according to standard procedures (19). The majority of the yeast strains used in this study are listed in Table I. A set of deletion mutants disrupted for putative oxidoreductases (Table II) was purchased from Research Genetics.

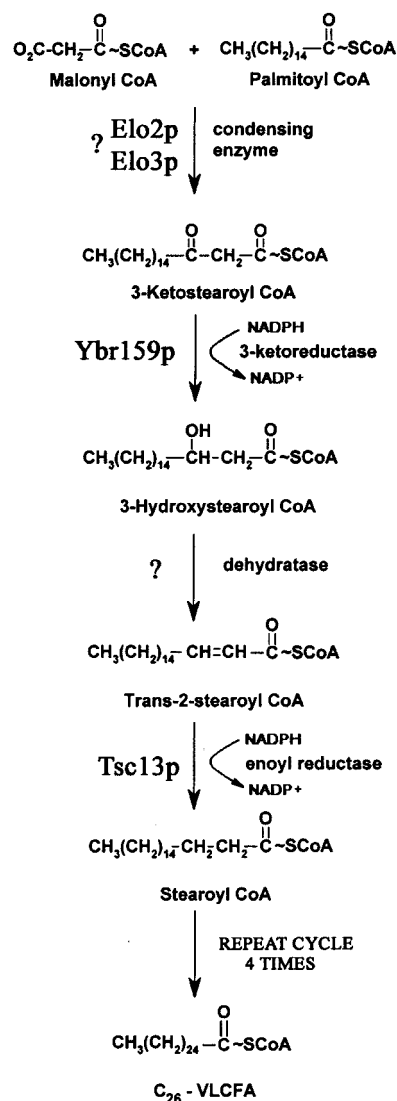To construct the *ybr159::TRP1*- and *ybr159::URA3*-disrupting al-

FIG. 1. **Pathway of fatty acid elongation.** Each cycle of elongation requires four successive reactions and lengthens the growing fatty acid by two carbon units: condensation of malonyl-CoA with the acyl-CoA substrate, reduction of the 3-ketoacyl-CoA, dehydration of the 3-hydroxy acyl-CoA, and reduction of the *trans*-2,3-acyl-CoA. Although the intermediates and the product of the elongation cycle are shown as CoA derivatives, this has not yet been experimentally confirmed.

leles, a *Sal*I/*Xba*I-ended PCR fragment extending from 200 bp upstream of the start codon of YBR159w to 200 bp past the stop codon was generated using primer 159F (*Sal*I-ended 5′-ACAGCTGTCGACTATA-GAGATAATTGTAGG-3′) and 159R (*Xba*I-ended 5′-AGAGCTCTAGAT-GATATTCTGGAAAAGCA-3′). The fragment was ligated between the *Xho*I and *Xba*I sites of a Bluescript plasmid. The resulting plasmid was digested with *Xho*I to remove a 779-bp fragment extending from codon 93 past the end of the YBR159w coding sequence. A *Sal*I-ended *TRP1* (or *URA3*) fragment, generated by PCR, was ligated into the *Xho*I site at the deletion junction to generate the disrupting allele. The disrupting allele was liberated from the plasmid by digestion with *Kpn*I and *Not*I. The *ybr159::TRP1 elo3::URA3* double mutant was generated by transforming the *Kpn*I/*Not*I-ended *ybr159w::TRP1*-disrupting fragment into strain TDY 2054 (*elo3::URA3*) (16) and selecting tryptophan prototrophs. The replacement of the *YBR159w* allele by the *ybr159::TRP1* allele was verified by PCR analysis. The *ybr159w::TRP1 tsc13-1* double mutant was generated by crossing a *ybr159w::TRP1* haploid mutant (TDY 1590, generated by disrupting YBR159w in TDY 2039) with TDY 2051a (*tsc13-1*) (16). The resulting diploid was sporulated, and following tetrad dissection, the products of meiosis that were the *ybr159w::TRP1 tsc13-1* double mutants were identified as tryptophan prototrophs that were unable to grow at 37 °C.

The *ypc1::kanMX*-disrupting allele was generated by PCR using

TABLE I
Strain list

Strain name	Genotype
TDY 2037	*Matα ura3–52 leu2 trp1 lys2*
TDY 2053	*Mata his4 ura3 trp1 leu2 elo2::URA3*
TDY 2054	*Matα elo3::ura3 his4–619 ura3–52 trp1 leu2*
TDY 2057	*Matα ade2 ura3 trp1 leu2 lys2 elo2::TRP1 tsc13–1*
TDY 2058	*Matα ade2 ura3 trp1 leu2 lys2 elo3::TRP1 tsc13–1*
TDY 1590	*Matα ybr159::TRP1 ura3–52 trp1 leu2 lys2*
TDY 2051a	*Mata tsc13–1 ura3–52 trp1 leu2*
TDY 1591	*Matα ybr159::TRP1 tsc13–1 ura3–52 trp1 leu2 lys2*
TDY 1593	*Matα ybr159::TRP1 elo3::URA3 ura3–52 trp1 leu2 lys2*
TDY 2302	*Matα ura3–52 trp1 lys2 csg2::URA3*
TDY 1592	*Mata ura3–52 trp1 leu2 lys2 his4 ybr159::TRP1 csg2::LEU2*
TDY 5999	*Mata ura3–52 leu2 trp1 ade2 elo2::TRP1*
TDY 6000	*Matα ura3–52 leu2 trp1 lys2 ypc1::kanMX ydc1::URA3*
TDY 6001	*Matα ura3–52 leu2 trp1 lys2*
TDY 6002	*Matα ura3–52 leu2 trp1 lys2 ade2 ypc1::kanMX*
TDY 6003	*Matα ura3–52 leu2 trp1 lys2 ydc1::URA3*
TDY 6004	*Matα ura3–52 leu2 trp1 ade2 ypc1::kanMX ydc1::URA3*
TDY 6005	*Mata ura3–52 leu2 trp1 lys2 elo2::TRP1*
TDY 6006	*Mata ura3–52 leu2 trp1 ade2 elo2::TRP1 ypc1::kanMX*
TDY 6007	*Mata ura3–52 leu2 trp1 elo2::TRP1 ydc1::URA3*
TDY 6008	*Mata ura3–52 leu2 trp1 ade2 elo2::TRP ypc1::kanMX ydc1::URA3*

TABLE II
Candidate genes responsible for residual 3-ketoreductase activity in the ybr159Δ mutant

Gene	Homology to Ybr159p
YMR226c	Score = 171 Identities = 69/212 (32%), Positives = 102/212 (48%)
YIL124w/AYR1[a]	Score = 118 Identities = 44/183 (24%), Positives = 85/183 (46%)
YIR036c	Score = 108 Identities = 51/212 (24%), Positives = 92/212 (43%)
YKL055c/OAR1[b]	Score = 70 Identities = 25/106 (23%), Positives = 53/106 (50%)
YDL114w	Score = 91 Identities = 34/125 (27%), Positives = 60/125 (48%)

[a] Ref. 18.
[b] Ref. 34.

genomic DNA prepared from the Research Genetics strain harboring the disruption and the *Eco*RI-ended YPC1F (5′-CCCGG̲G̲G̲A̲T̲C̲C̲GC-CGATTAGATCCGGCCC) and *Xba*I-ended YPC1R (5′-CCGGGCTC-GAGCATGTCCCGAATTAGCTA) primers. Construction of the *ydc1*::*URA3*-disrupting allele (kindly provided by the Obeid laboratory) was described earlier (20). The *YPC1* and *YDC1* genes were sequentially disrupted in TDY 2037 to generate TDY 6000, which was crossed to TDY 2053 (*elo2*Δ). This diploid was sporulated, and the tetrads were dissected to generate the set of haploid strains (TDY 6001–6008) having the various combinations of the *ypc1*::*kanMX*, *ydc1*::*URA3*, and *elo2*Δ mutations (Table I).

Construction of Ybr159p-GFP by Chromosomal Fusion—Chromosomal C-terminal GFP fusion to Ybr159p was performed by the short flanking homology method (21). In brief, coding sequences for GFP and the kanMX6 selection marker were amplified from template plasmid pFA6a-GFPS65T-kanMX6 (provided by J. Hegemann, Heinrich-Heine-Universität, Düsseldorf, Germany) using hybrid primers homologous to 30 or 26 bp 5′ or 3′ of the template plasmid, respectively, and 50 nucleotides upstream or downstream of the chromosomal integration sites, flanking the stop codon. The following primers were used (letters in boldface type mark the vector sequences): *YBR159* upstream primer, 5′-CTATCAGAATTAGAGCCTTAAAAAAAGCCGCAAGACAGGTTAA-AAAGGAA**GGAGCAGGTGCTGGTGCTGGTGCTGGAGCA**-3′; *YBR159* downstream primer, 5′-ATATATATATATATATGTATTGTAT-AAAAACTATCTCGAGAACGATAATT**ATCGATGAATTCGAGCTC-GTTTAAAC**-3′. After transformation of the linear fragments into FY1679 (*MAT**a**/α ura3–52/ura3–52 trp1Δ/TRP1 leu2Δ/LEU2 his3Δ/HIS3 GAL2/GAL2*) and selection of Geneticin-resistant colonies, cells were sporulated, and haploid strains containing the GFP-tagged alleles were selected. Growth tests in the presence of inhibitors of fatty acid synthesis/elongation (cerulenin, soraphen A (22), and calcium) and at elevated or reduced temperatures did not unveil any changes compared with wild type, demonstrating that the GFP-tagged fusion allele of YBR159w was fully functional.

The pYES-AT-159 Plasmid—An *Arabidopsis thaliana* expressed se-

quence tag (GenBank™ accession number AA10E08; kindly provided by Prof. H. J. Bohnert, University of Arizona) derived from gene F12A21.31 was used as template DNA for PCR amplification using primers YAt159.for (5′-GCG̲G̲G̲T̲A̲C̲C̲ACCATGGAGATCTGCACTTAC-3′) and YAt159.rev (5′-GCG̲G̲A̲G̲C̲T̲C̲TCATTCTTTCTTCATGGA-3′). The amplified sequence was then restricted using *Kpn*I and *Sac*I (underlined in the forward and reverse primers, respectively), purified using the Qiagen PCR purification kit, and ligated into the *Kpn*I and *Sac*I sites of the pYES2 plasmid (Invitrogen).

Ceramide, Long-chain Base, and Fatty Acid Analyses—Ceramides were extracted and analyzed by thin layer chromatography (TLC) as previously described (23). Ceramides were purified by preparative silica gel TLC and subjected to acid methanolysis, and the fatty acid methyl esters (FAMEs) and long-chain bases (LCBs) were recovered as described earlier (23). LCBs were extracted, separated by TLC, and visualized using ninhydrin as described (15). Fatty acids were extracted, and the FAMEs were prepared as previously described (16). Gas chromatography/mass spectrometry (GCMS) was performed using an HP 6890 Series GC system with a Supelcowax 10 column, coupled to an HP 5973 Mass Selective Detector.

Elongase Assays—Microsomes were prepared from the wild-type or mutant cells as has been previously described (24). Total elongase activity was measured in a volume of 200 μl containing 50 mM Tris, pH 7.5, 1 mM MgCl$_2$, 150 μM Triton X-100, 1 mM NADPH, 1 mM NADH, 10 mM β-mercaptoethanol, 40 μM palmitoyl-CoA, and 60 μM [2-^{14}C]malo-nyl-CoA (0.05 μCi/ml) at 37 °C. The reaction was initiated by the addition of 0.3–1.0 mg of microsomal protein. Protein concentrations were determined using the Bio-Rad protein assay reagent. For assays of only the condensing activity, the NADPH and NADH were omitted. At the indicated times, the reaction was terminated by adding 200 μl of 5 M KOH, 10% MeOH and heating at 80 °C for 1 h. Following the addition of 200 μl of 10 N H$_2$SO$_4$, fatty acids were recovered by two 1.5-ml extractions into hexane. The extracted fatty acids were resolved by silica gel TLC using hexane/diethyl ether/acetic acid (30:70:1) as the developing solvent. The radiolabeled fatty acids were detected and

quantified using a PhosphorImager SI (Amersham Biosciences).

Serine Palmitoyltransferase (SPT) Assays and Immunoblotting of Lcb1p and Lcb2p—The SPT assays were preformed as previously described (24), except that 0.4 mg of microsomal protein and 75 μM palmitoyl-CoA were used. Each assay was conducted in quadruplicate, and the average SPT activity is reported. The methods used for immunoblotting and for detection of Lcb1p and Lcb2p with the anti-Lcb1p and anti-Lcb2p antibodies were also previously described (24).

Immunoprecipitation—Microsomes were prepared from strains containing Ybr159p-GFP and Tsc13p-MYC or containing Ybr159p-GFP, Tsc13p-MYC, and Elo3p-HA. The microsomes were solubilized at 1 mg/ml with 2 mM sucrose monolaurate (Roche Molecular Biochemicals) for 10 min, and the high speed ($1 \times 10^5 \times g$, 30 min) supernatant was collected. The supernatant (150 μl) was incubated with 25 μl of the precipitating antibody (0.5 mg/ml) coupled to Sepharose (from Babco, Berkeley, CA) for 2 h. The precipitates were washed three times with 600 μl of 50 mM HEPES, pH 7.5, and resuspended in 150 μl of SDS loading buffer, and a 10-μl sample was subjected to 8% SDS-PAGE. Following transfer of the separated proteins to nitrocellulose, the blots were blocked in 0.1 M Tris, pH 7.5, 0.15 M NaCl, 0.1% Tween 20, 5% dry milk. The Tsc13p-Myc was detected with horseradish peroxidase-conjugated monoclonal anti-Myc antibodies (from Invitrogen) at 1:5000. Elo3p-HA was detected using horseradish peroxidase-conjugated monoclonal anti-HA antibodies (from Roche Molecular Biochemicals) at 1:1000. The bound antibodies were detected by the ECL Western blotting detection system (Amersham Biosciences).

Immunofluorescence and Fluorescence Microscopy—Immunostaining of protein in yeast cells was performed as described (25) with the following modifications. The cells harboring the Ybr159p-GFP chromosomal fusion were transformed with plasmids expressing Elo3p-HA, Elo2p-HA, or Tsc13p-MYC (the construction of these plasmids was described previously (16)). The cells were fixed with 4% methanol-free formaldehyde in PBS for 2 h at room temperature. Cells were permeabilized in phosphate-buffered saline containing 0.1% Triton X-100, 0.05% saponin, 10 mM glycine, and 0.1% bovine serum albumin. Before adding antibody, the digested cells were blocked by incubating in 10% of bovine serum albumin for 30 min. For detecting Elo3p-HA or Elo2p-HA, the cells were incubated with anti-HA rhodamine antibody (Roche Molecular Biochemicals) at 2 μg/ml in phosphate-buffered saline containing 1.0% bovine serum albumin, 0.1% Tween 20 for 2 h. For detecting Tsc13p-MYC, cells were incubated with a monoclonal anti-MYC antibody (from Invitrogen; 1:200 dilution) followed by the Cy3-conjugated anti-mouse IgG secondary antibody (Sigma; 1:5000). Fluorescence microscopy was performed on an IX70 inverted fluorescence microscope (Olympus) equipped with a HiQ fluorescein filter set (for GFP, excitation/emission was 460–490 nm/510 nm; for rhodamine and Cy3, excitation/emission was 510–550 nm/590 nm) and a Planapochromatic $\times$100 oil immersion objective lens and a 100-watt mercury lamp. Images were collected with a Princeton Instruments 5-MHz MicroMax cooled CCD camera, a shutter and controller unit, and IPLab software (version 3.5; Scanalytic Co.). Signals from the fluorescein isothiocyanate (Ybr159-GFP) and rhodamine and Cy3 fluorescence channels were merged to unveil colocalization of signals.

RESULTS

Deletion of the YBR159w Gene Causes Slow Growth, Suppression of the Ca^{2+}-sensitive Phenotype Associated with the csg2Δ Mutation, and Synthetic Lethality with the elo2Δ Mutation—The Ybr159p protein was previously shown to be required for C2 elongation of polyunsaturated fatty acids mediated by heterologous expression of a *C. elegans* polyunsaturated fatty acid-elongating activity F56H11.4 activity in *S. cerevisiae* (11). The Ybr159p requirement for polyunsaturated fatty acid elongation along with its homology to oxidoreductases suggested that it is the 3-ketoreductase activity of the endogenous elongase system in yeast. However, whereas the role of Ybr159p in heterologous fatty acid elongation has been demonstrated, whether or not it functions in endogenous elongation remained to be determined. The role of Ybr159p in the synthesis of endogenous VLCFAs is addressed in this study.

The *ybr159Δ* mutant cells grow very slowly, especially upon germination from spores (Fig. 2A) and when growing at elevated temperature (*e.g.* 37 °C) (11) (Fig. 2B). The presumptive *Arabidopsis thaliana* homolog (F12A21.31; designated At-
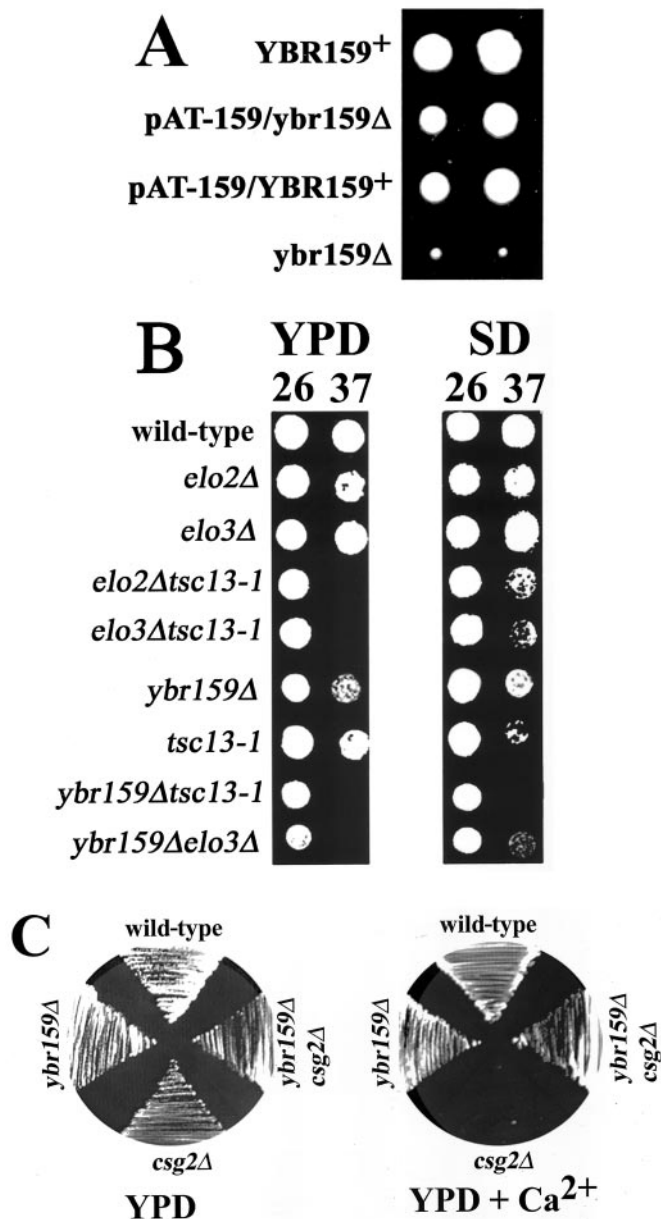
FIG. 2. **The *Ybr159Δ* mutation causes slow growth, synthetic lethality with the *elo2Δ* mutation, and suppression of the Ca^{2+}-sensitive phenotype caused by the *csg2Δ* mutation.** *A*, a heterozygous *ybr159::TRP1/YBR159$^+$* diploid that had been transformed with a p-YES-URA3 plasmid carrying the *Arabidopsis thaliana YBR159w* homolog (F12A21.31) was sporulated and dissected on YPD agar plates. The plates were incubated at 26 °C for 7 days and then photographed. Subsequent analysis revealed which spores had the wild-type *YBR159$^+$* gene, which had the *ybr159::TRP1*-disrupted gene, and which harbored the plasmid. The spore colonies from two representative tetrads are shown. *B*, the growth phenotypes of the elongase single and double mutants are shown. The indicated strains were grown in YPD medium to an A_{600} of 0.1 and were diluted into the wells of a microtiter plate. The cells were transferred to either YPD or SD plates, and the plates were incubated at 26 °C for 3 days or 37 °C for 2 days. The *ybr159Δelo2Δ* double mutant is missing because it is inviable. *C*, the *ybr159Δ* mutation suppresses the calcium sensitivity of the *csg2Δ* mutant. The indicated strains were streaked onto YPD agar plates with or without 50 mM CaCl$_2$, and the plates were incubated at 26 °C for 3 days. The *ybr159Δcsg2Δ* double mutant is far less sensitive to calcium than the *csg2Δ* single mutant.

YBR159) of the *S. cerevisiae YBR159w* gene complemented the deficiency in the heterologous microsomal elongation activity associated with the *ybr159Δ* mutation (11). Heterologous expression of the At-Ybr159p also complemented the slow growth

phenotype of the *ybr159Δ* mutant spores (Fig. 2*A*), demonstrating that the *Arabidopsis* gene also compensated for the endogenous (presumed VLCFA synthesis) defect that conferred slow growth.

Mutations in the other known elongase genes (*ELO2*, *ELO3*, and *TSC13*) suppress the Ca^{2+}-sensitive phenotype of the *csg2Δ* mutation (16). The *csg2Δ* mutant accumulates high levels of inositolphosphoceramide (IPC) due to failure to mannosylate IPC (17, 26). The accumulation of IPC confers Ca^{2+} sensitivity, and mutants that reduce IPC levels suppress the Ca^{2+}-sensitive phenotype (15). In wild-type yeast, all ceramides and sphingolipids contain C26-VLCFA; therefore, mutations that reduce fatty acid elongation reduce the levels of IPC and thereby suppress the Ca^{2+} sensitivity conferred by the lack of Csg2p. As would be expected if Ybr159p is required for endogenous VLCFA synthesis, the *ybr159Δcsg2Δ* double mutant was far less Ca^{2+}-sensitive than the *csg2Δ* single mutant (Fig. 2*C*).

We also investigated whether combining the *ybr159Δ* mutation with other elongase mutations would result in synthetic growth phenotypes. For these studies, we crossed a *ybr159Δ* mutant with a mutant harboring a second elongase mutation (the *elo2Δ*, the *elo3Δ*, or the *tsc13-1* mutation) to generate the doubly heterozygous diploids. The products of meiosis were analyzed following sporulation and tetrad dissection. We found that the combination of the *ybr159Δ* mutation with an *elo2Δ* mutation was synthetically lethal, since all of the spores (from 16 tetrads) that could be deduced to have inherited both mutations (the *ybr159Δelo2Δ* double mutant spores) failed to germinate (data not shown). The *ybr159Δelo3Δ* and the *ybr159Δtsc13-1* double mutants were both viable, but they grew more slowly, especially at elevated temperatures, than the single mutants (Fig. 2*B*).

The ybr159Δ Mutant, Like Other Elongase Mutants, Accumulates Long-chain Bases and Medium-chain Ceramides— In previous studies, we found that mutants with defects in VLCFA synthesis accumulated very high levels of the free LCBs, phytosphingosine (PHS) and dihydrosphingosine (16). This phenotype is also observed for the *ybr159Δ* mutant (Fig. 3*A*). The accumulation of high levels of free LCBs in the elongase mutants does not reflect reduced partitioning of the LCBs into ceramides due to the VLCFA deficiency. Rather, the elongase mutants accumulate significant levels of medium-chain ceramides containing PHS (discussed below), and thus the total LCB levels (free LCBs and LCBs incorporated into ceramides and sphingolipids) are increased in the mutants.

The elevated LCB pool suggested an increased rate of synthesis of the LCBs in the elongase mutants. Therefore, we tested whether serine palmitoyltransferase (SPT), the committed and presumed rate-limiting enzyme of LCB synthesis, was up-regulated in the elongase mutants. The abundance of the Lcb1p and Lcb2p subunits of SPT was similar in microsomes prepared from wild-type and elongase mutant cells (Fig. 3*B*). We also measured SPT activity in microsomes prepared from wild-type and elongase mutant microsomes and found no increase in the *in vitro* SPT activity for the elongase mutants (Fig. 3*C*). These experiments indicate that the elevated LCBs do not result from increased expression of the SPT enzyme. It is possible that the reduced partitioning of palmitoyl-CoA (a common substrate for SPT and the condensing enzyme of the elongase system) into the elongase pathway results in enhanced LCB synthesis by providing higher substrate pools for SPT. However, this is not likely, because a similar LCB-accumulating phenotype is reported for the *lac1Δlagl Δ* mutant cells, but in this case the VLCFA levels are also elevated (27, 28) (see "Discussion").
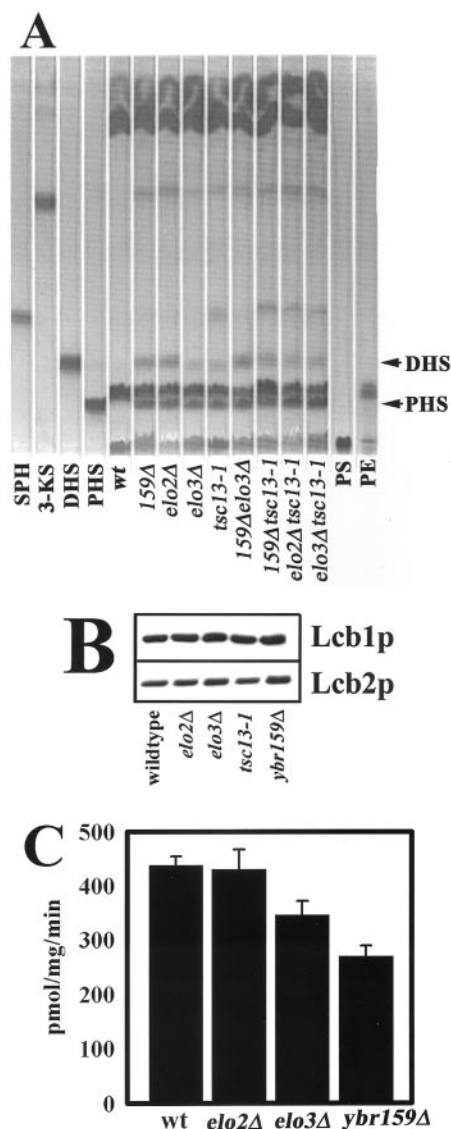
FIG. 3. **Similar to the other elongase mutants, the *ybr159Δ* mutant accumulates high levels of LCBs.** *A*, LCBs were extracted from 10 A_{600} units of the indicated cells, separated by TLC, and visualized by ninhydrin staining. The LCB standards sphingosine (*SPH*), 3-ketosphingosine (*3-KS*), dihydrosphingosine (*DHS*), and phytosphingosine (*PHS*) were spotted in *lanes 1–4* as indicated. The ninhydrin-reactive species that migrate just above PHS and near the origin are phosphatidylethanolamine (*PE*) and phosphatidylserine (*PS*) (see standards, *lanes 14* and *15*). *B*, the elevated LCB levels in the elongase mutants do not result from increased expression of the Lcb1p or Lcb2p subunits of SPT. Ten μg of microsomal proteins from the indicated strains were resolved by SDS-PAGE electrophoresis, transferred to nitrocellulose, and subjected to Western blot analysis using affinity-purified polyclonal anti-Lcb1p and anti-Lcb2p antibodies as previously described (33). *C*, the *in vitro* SPT activity, measured using microsomes from the indicated elongase mutants (33), is similar to the activity in microsomes from the wild-type (*wt*) cells.

Whereas the ceramide (C-ceramide) in wild-type cells contains PHS and α-OH-C26 fatty acids, the elongase mutants also accumulated significant levels of ceramides with shorter chain fatty acids, and these fatty acids were also α-hydroxylated (16). These medium-chain (relatively hydrophilic) ceramides also accumulated in the *ybr159Δ* mutant (Fig. 4*A*). The presumptive medium-chain ceramides were eluted from the TLC plate and subjected to acid methanolysis, and the resultant LCBs (by TLC) and FAMEs (by GCMS) were analyzed. The ceramides were composed of PHS and α-OH-C16 fatty acids
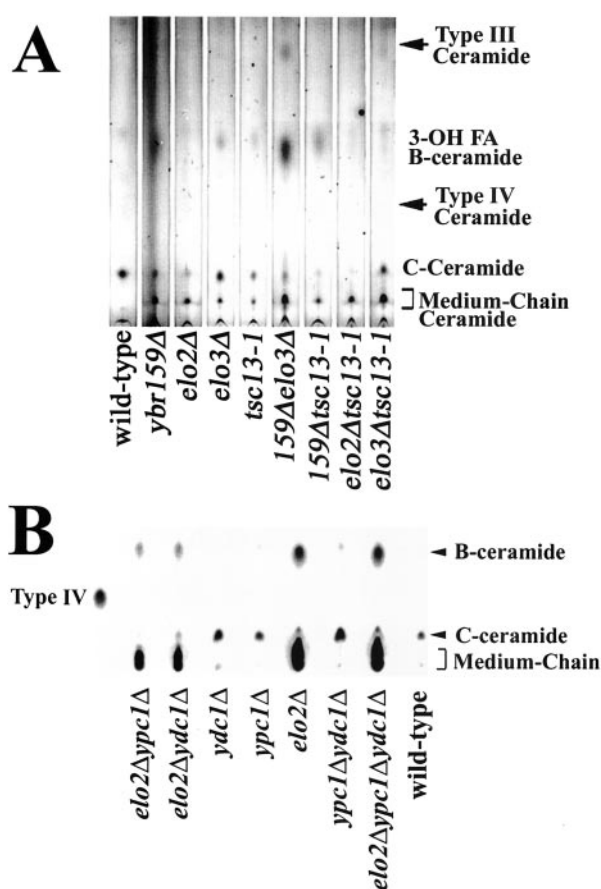
FIG. 4. **The elongase mutants accumulate medium-chain ceramides: Synthesis of the medium-chain ceramides is not mediated by the Ypc1p and/or Ydc1p ceramidases.** *A*, ceramides were extracted from 10 A_{600} units of the indicated cells, separated by TLC, and visualized by charring (23). Bovine ceramide type III (consisting of sphingosine and C16-FA) and type IV (consisting of sphingosine and α-OH-C16-FA) standards run at the indicated positions. The major ceramide in wild-type cells (C-ceramide) consists of PHS and α-OH-C26-FA. The elongase mutants have reduced C-ceramide, and they accumulate high levels of relatively hydrophilic ceramides that are composed of PHS and α-OH-C16-FA (the medium-chain ceramides). *B*, ceramides from 12.5 A_{600} units of the indicated strains were extracted and analyzed by TLC. In this case, the ceramides were analyzed by UV light after spraying the plates with 1% 8-anilino-1-napthalenesulfonic acid. The deletion of *YPC1* (*lane 3*), *YDC1* (*lane 4*), or both *YPC1* and *YDC1* (*lane 9*) did not prevent the medium-chain ceramides from accumulating in the *elo2Δ* mutant. The medium-chain ceramides from the *bracketed region* were eluted from the TLC plate and subjected to acid methanolysis, and the FAMEs and LCBs that were produced were recovered and analyzed.

(data not shown). A small amount of ceramide that was unhydroxylated on the C16 fatty acid (labeled *B-ceramide* in Fig. 4*A*) was also present and migrated in the TLC between the type III (unhydroxylated) and type IV (hydroxylated) bovine ceramide standards. In addition, a novel species that migrated similarly to the B-ceramide accumulated in the *ybr159Δ* mutant (Fig. 4*A*). This species was found to be a 3-OH fatty acid (discussed below).

These medium-chain ceramides might be synthesized by the acyl-CoA-dependent ceramide synthase activity; however, in wild-type cells, this enzyme appears to have high selectivity for C26 fatty acyl CoA, despite the relatively high intracellular level of C16 fatty acids. Alternatively, the medium-chain ceramides could arise from the reversal of a ceramidase activity, possibly driven by the high LCB levels in the elongase mutants. Two ceramidase-encoding genes, *YPC1* and *YDC1*, with specificity toward PHS-containing and dihydrosphingosine-contain-

ing ceramides respectively, have been identified in yeast (20, 29). To determine whether the accumulation of the medium-chain ceramides in the elongase mutants depends on Ypc1p and/or Ydc1p, the ceramides from an *elo2Δ* mutant, an *elo2Δypc1Δ* or an *elo2Δydc1Δ* double mutant, or an *elo2Δypc1Δydc1Δ* triple mutant were compared. The medium-chain ceramide accumulation caused by the *elo2Δ* mutation was not blocked by eliminating the ceramidase genes (Fig. 4*B*). The medium-chain ceramides from these strains were purified and hydrolyzed by acid methanolysis, and again the LCB moiety of these ceramides was found to be PHS, and the fatty acid moiety was found to be predominantly α-OH-C16 (data not shown). Since deleting either *YPC1* and/or *YDC1* did not prevent the accumulation of the medium-chain ceramides, they are most likely synthesized by the acyl-CoA-dependent ceramide synthase. This raises the question of why ceramide synthase, which normally displays high selectivity for C26-acyl-CoA, uses palmitoyl-CoA in the elongase mutants (see "Discussion").

These results show that the LCB- and medium-chain ceramide-accumulating phenotypes previously found to be characteristic of elongase mutants are also observed for the *ybr159Δ* mutant and support a role for Ybr159p in endogenous VLCFA synthesis. In addition, they demonstrate that the high levels of LCBs in the mutants do not result from increased expression of the Lcb1p and/or Lcb2p subunit of SPT. Finally, the medium-chain ceramides that accumulate in the elongase mutants do not depend on the presence of the ceramidases, Ypc1p or Ydc1p.

In Vivo and in Vitro Assays of VLCFA Synthesis Confirm a Deficiency in the ybr159Δ Mutant—Fatty acids from wild-type, *ybr159Δ*, *ybr159Δtsc13-1*, and *ybr159Δelo3Δ* cells were extracted and analyzed by GCMS (see "Experimental Procedures"). As shown in Fig. 5, there was a significant reduction in the levels of the C26 fatty acids in cells harboring the *ybr159Δ* mutation. In addition, several fatty acid species were observed in the mutants that were not present in wild-type cells, including α-OH-C16 fatty acid. As discussed above, the elongase mutants synthesize ceramides that have C16 fatty acids, whereas in wild-type cells the ceramides have exclusively C26 fatty acids. These medium-chain ceramides are substrates for the α-hydroxylating enzyme, Scs7p, and thereby generate the α-OH-C16 fatty acids (16, 23). Thus, the accumulation of the α-OH-C16 fatty acids in the *ybr159Δ* mutant reflects the accumulation of the medium-chain ceramides, a phenotype diagnostic of a VLCFA synthesis deficiency.

In addition to the α-OH-C16 fatty acids, the *ybr159Δ* mutant cells also accumulated 3-OH fatty acids of different chain lengths (C16, C18, and C20). There are no known enzymes that hydroxylate fatty acids or ceramides at C3; rather, these fatty acids are presumed to be intermediates of the elongation pathway (Fig. 1). As mentioned above, the 3-OH fatty acids from the *ybr159Δ* mutant were also observed on the ceramide TLC plates (see Fig. 4*A*). The accumulation of these 3-OH fatty acid species suggests that the *ybr159Δ* mutant is deficient in the dehydratase activity as well as in the 3-ketoreductase activity of the elongation system (discussed further below).

We previously assayed microsomes prepared from the *ybr159Δ* mutant for *in vitro* elongase activity (11). The first step of the elongation cycle is the condensation of malonyl-CoA with an acyl-CoA (*e.g.* palmitoyl-CoA) to form a 3-keto-acyl-CoA intermediate (Fig. 1). Omitting pyridine nucleotide from the assay mix prevents the reduction of the 3-keto-acyl-CoA intermediate and thereby allows the first step of elongation (condensation) to be measured (Fig. 6, *lane 1* of each *panel*). A time course of the overall elongation was measured in the presence of NADH/NADPH (Fig. 6, *lanes 2–4* of each *panel*).
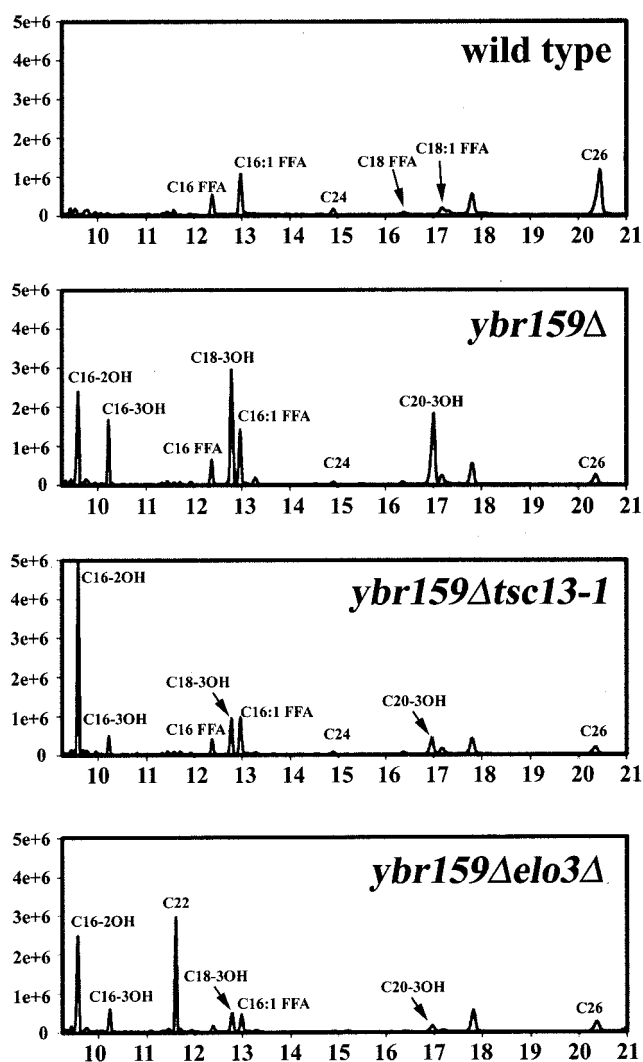
FIG. 5. **The *ybr159Δ* mutant cells are deficient in C26 fatty acids and accumulate 2-OH-C16 and 3-OH-C16, -C18, and -C20 Fatty Acids.** FAMEs were derived from the indicated strains and were analyzed by GCMS. The profile spanning retention times from 9 to 21 min is shown. An internal C17 standard (retention time, 8.8 min), added to the cells prior to the extraction, was used to normalize the data. A small percentage of the fatty acids were not methylated (labeled free fatty acids (*FFA*)).

Elongation intermediates did not accumulate during the elongation reactions catalyzed by the wild-type microsomes (Fig. 6a), which is consistent with previous studies of the rat microsomal elongating systems demonstrating that the condensation reaction is rate-limiting (30). However, when microsomes prepared from the *ybr159Δ* mutant were used in the assay, accumulation of the 3-keto-acyl and 3-hydroxyacyl intermediates was observed (11) (Fig. 6b). This is consistent with the defect in Ybr159p causing reduced activity of both the 3-ketoreductase and the dehydratase activity of the elongase system.

We had also previously assayed *in vitro* elongation using microsomes prepared from the *tsc13-1* mutant. In this case, accumulation of the trans-2,3-stearoyl and the 3-hydroxystearoyl intermediates was observed (16) (Fig. 6e). This is consistent with the defect in Tsc13p causing reduced activity of the *trans*-2,3-enoyl-CoA reductase leading to accumulation of the trans-2,3-stearoyl-CoA. Because the dehydratase step of elongation is reversible (31), accumulation of trans-2,3-stearoyl-CoA resulted in the observed accumulation of 3-hydroxystearoyl-CoA as well.

These previous studies were extended by comparing the elongase activity of microsomes prepared from mutants with various combinations of the elongase mutations (Fig. 6, *f–i*). These experiments confirmed our previous finding that when Ybr159p was missing, the 3-keto-acyl intermediate accumulated, consistent with Ybr159p being the major 3-ketoreductase activity of the microsomal yeast fatty acid elongase system. In addition, when Ybr159p was missing, the 3-OH-acyl intermediate of fatty acid elongation accumulated, indicating that the dehydratase activity was also compromised in the absence of Ybr159p. Significantly, when Tsc13p activity was deficient, the 3-OH-acyl intermediate accumulated in proportion to the trans-2,3-acyl intermediate, as would be expected if it arose from reversal of the dehydratase activity. On the other hand, when Ybr159p was missing, there was a large increase in the 3-OH-acyl intermediate with no concomitant accumulation of the trans-2,3-acyl intermediate. This indicates that when Ybr159p is missing, the forward dehydratase activity is decreased to cause the 3-OH-acyl intermediate to accumulate, whereas when Tsc13p is missing, the reverse dehydratase activity is increased to cause the 3-OH-acyl intermediate to accumulate.

The *in vitro* elongase activity measured using the microsomes from the *elo2Δ* (Fig. 6c) and *elo3Δ* (Fig. 6d) single mutants appeared very similar to that with the wild-type microsomes, in that no intermediates accumulated. However, the condensation activity in the *elo2Δ* mutant was reduced about 3-fold (Fig. 6c), consistent with Elo2p being required for efficient condensation of palmitoyl-CoA with malonyl-CoA. The reduced overall elongation in both the *elo2Δ* and the *ybr159Δ* mutants is also consistent with the observation that the *elo2Δybr159Δ* double mutant is inviable. Although the *elo3Δybr159Δ* double mutant accumulates both the 3-keto and the 3-OH acyl intermediates, less 3-keto intermediate forms than in the *ybr159Δ* single mutant (Fig. 6f). This suggests that the 3-keto intermediate that is formed by Elo2p (since Elo3p is missing) is reduced more efficiently by an alternative 3-ketoreductase than the 3-keto intermediate formed by Elo3p, but this requires further investigation. The *ybr159Δ* mutation does not prevent the accumulation of the *trans*-2,3-enoyl intermediate in the *ybr159Δtsc13-1* double mutant; nor does the *tsc13-1* mutation prevent the high 3-OH acyl intermediate associated with the *ybr159Δ* mutation from accumulating (Fig. 6g).

In summary, the accumulation of the 3-ketoacyl intermediate (*in vitro*) and the 3-OH acyl intermediate (both *in vivo* and *in vitro*) indicate that both the 3-ketoreductase and the dehydratase activities are compromised in the *ybr159Δ* mutant. The accumulation of these intermediates is not blocked by the *elo3Δ* mutation or by the *tsc13-1* mutation. The synthetic lethal phenotype of the *elo2Δybr159Δ* double mutant indicates that the reduced overall elongation observed by either single mutant is additive, making the double mutant unable to synthesize sufficient VLCFAs for viability.

The Ybr159p Protein Resides in the Endoplasmic Reticulum, Co-localizes with Tsc13p and Elo3p, and Also Co-immunoprecipitates with Tsc13p and Elo3p—Tsc13p, Elo3p, and Elo2p all displayed a perinuclear and peripheral staining consistent with localization to the ER (16, 32). Furthermore, Tsc13p was found to co-immunoprecipitate with Elo2p and with Elo3p, indicating that the elongase proteins are organized in a complex. We next addressed whether Ybr159p co-localizes with and associates with the other elongase proteins. Ybr159p has a canonical dilysine ER retention motif, which along with its homology to the oxidoreductases, was the criterion used to identify it as a potential 3-ketoreductase of the elongase system (11). In addition, all enzymes involved in fatty acid elongation
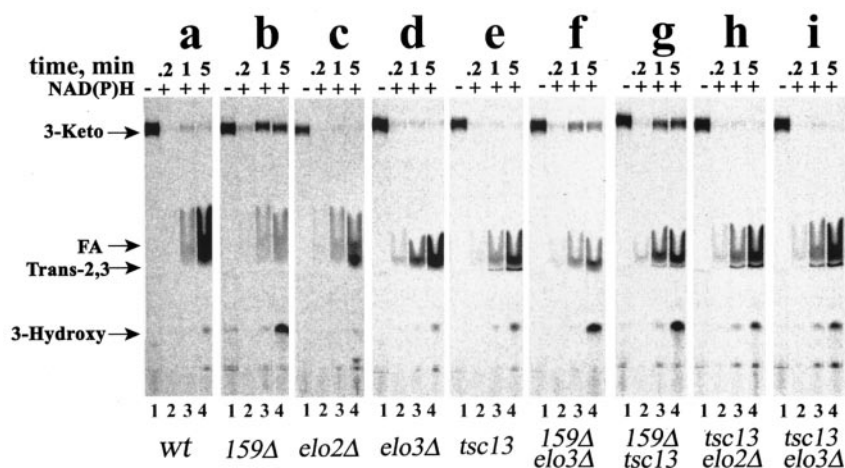
FIG. 6. **The *ybr159Δ* mutant cells have normal condensation activity but are deficient in 3-ketoreductase and dehydratase activity.** Fatty acid elongation activity in microsomes prepared from the indicated strains was compared using C16-CoA as a substrate by measuring the incorporation of radiolabeled malonyl-CoA into hexane-extractable fatty acids. The assays were conducted in the absence of NADPH/NADH for 5 min to measure condensation activity (*lane 1* of each set). NADPH/NADH was included in the reactions measuring total elongation for 0.2 (*lane 2*), 1.0 (*lane 3*), or 5.0 (*lane 4*) min. The reactions were stopped at the indicated times, and the fatty acids were extracted and separated by TLC. The positions of the 3-ketostearate (*3-Keto*), stearate (*FA*), *trans*-2,3-stearate (*Trans-2,3*), and 3-hydroxystearate (*3-Hydroxy*) intermediates were determined by running the standards on the TLC plate and charring after exposure to PhosphorImager screens.

identified so far have very basic pI values (>9) and several transmembrane domains, which is also characteristic for Ybr159p.

To analyze subcellular localization, Ybr159p was C-terminally tagged with GFP by chromosomal fusion (see "Experimental Procedures"). The Ybr159p-GFP tagged protein was functional because the strain grew normally, and the 2-OH and 3-OH fatty acids (diagnostic of an elongase defect) did not accumulate. Indeed, localization studies of Ybr159p-GFP confirmed that it localizes to the nuclear/peripheral ER membrane (Fig. 7*A*, *panel a*). The Ybr159-GFP protein co-localizes with Elo3p-HA (Fig. 7*A*, *panel b*), Elo2p-HA (Fig. 7*A*, *panel c*), and Tsc13p-Myc (Fig. 7*A*, *panel d*). The epitope-tagged proteins were detected by immunofluorescence using either rhodamine-conjugated anti-HA (for Elo3p and Elo2p) or Cy3-conjugated anti-Myc (for Tsc13p-Myc) antibodies. Detailed microscopic analyses of GFP-tagged Ybr159p unveiled exclusive ER localization throughout various growth phases and no enrichment in the nuclear-vacuolar junctions (not shown). Thus, the physiological relevance of an enrichment of one component of the microsomal fatty acid complex, Tsc13p, to nuclear-vacuolar junctions remains obscure (16).

For the immunoprecipitation experiments, solubilized microsomes were prepared from cells that were co-expressing Tsc13p-Myc and Ybr159p-GFP either with or without Elo3p-HA (Fig. 7*B*). As we reported previously, the anti-HA antibodies pulled down Tsc13p-Myc, and the anti-Myc antibodies pulled down Elo3p-HA when Tsc13p-Myc and Elo3p-HA were co-expressed (Fig. 7*B*). These experiments also indicated that Ybr159p-GFP associates with the Elo3p-HA/Tsc13p-Myc-containing complexes, since anti-GFP antibodies pulled down Tsc13p-Myc and Elo3p-HA (Fig. 7*B*). Whether or not Ybr159p co-immunoprecipitates with Elo2p has not yet been tested.

The Residual 3-Ketoreductase Activity in the Ybr159Δ Mutant Is Likely to Depend on the AYR1 Gene Product—The results reported above indicate that the *YBR159w* gene encodes the major 3-ketoreductase activity of the yeast elongase system of enzymes. However, it cannot be the only gene that encodes such an activity, because there is residual VLCFA synthesis in the *ybr159Δ* mutant (Fig. 5). Furthermore, other mutants that fail to synthesize VLCFAs (the *tsc13Δ* mutant and the *elo2Δelo3Δ* double mutant) are inviable, whereas the *ybr159Δ* mutant grows, albeit slowly. Therefore, we investigated

whether any of the genes most closely related to *YBR159w* was likely to encode the residual 3-ketoreductase activity. We reasoned that disruption of the gene that encodes the residual 3-ketoreductase activity would be lethal in combination with the *ybr159Δ* mutation. There are several other putative oxidoreductase-encoding genes in yeast that display homologies to the *YBR159w* gene (11) (Table II). We obtained the set of haploid disruptant mutants in which each of these genes had been replaced with the kanMX resistance marker (from Research Genetics) and crossed them to the haploid *ybr159::URA3* mutant. For four of five candidates, Geneticin-resistant uracil-prototrophic segregants of the heterozygous diploid strains were recovered, indicating that the double mutants were viable. However, for the diploid that was heterozygous for the *yil124w/ayr1::kanMX* and the *ybr159::URA3* mutations, no viable Geneticin-resistant uracil-prototrophic meiotic segregants were recovered. Therefore, disruption of the *AYR1* gene was demonstrated to be synthetically lethal with the *ybr159Δ* mutation. In a previous study (18), spores harboring the *ayr1Δ* mutation were found to be unable to germinate, raising the possibility that the *AYR1* gene was not disrupted in the strain purchased from Research Genetics. However, we confirmed the *ayr1::kanMX* disruption in this strain by PCR. In our studies, the *ayr1::kanMX* single mutant spores germinated as well as wild type; this phenomenon may be related to differences in the construction of the disrupting allele or in the yeast strains.

To further investigate the possibility that Ayr1p catalyzes 3-ketoreductase activity in the *ybr159Δ* mutant, we addressed whether overexpression of Ayr1p would suppress the slow growth phenotype of *ybr159Δ* mutant spore colonies. However, a high copy number (pRS424-*TRP1*-based) *AYR1*-containing plasmid did not suppress the slow growth of *ybr159Δ* mutant spore colonies. The *ayr1::kanMX* mutant was also analyzed for elongase phenotypes. However, the mutant did not accumulate LCBs or medium-chain ceramides. Furthermore, *in vivo* fatty acid analyses and *in vitro* elongase assays did not reveal any evidence of a VLCFA synthesis defect in the *ayr1Δ* mutant. Finally, the *ayr1Δ* mutation was not synthetically lethal with the *elo2Δ* or the *elo3Δ* mutation. Therefore, although the synthetic lethality of the *ayr1Δ ybr159Δ* double mutant suggests that Ayr1p provides the residual 3-ketoreductase activity in the *ybr159Δ* mutant, the lack of elongase phenotypes in the
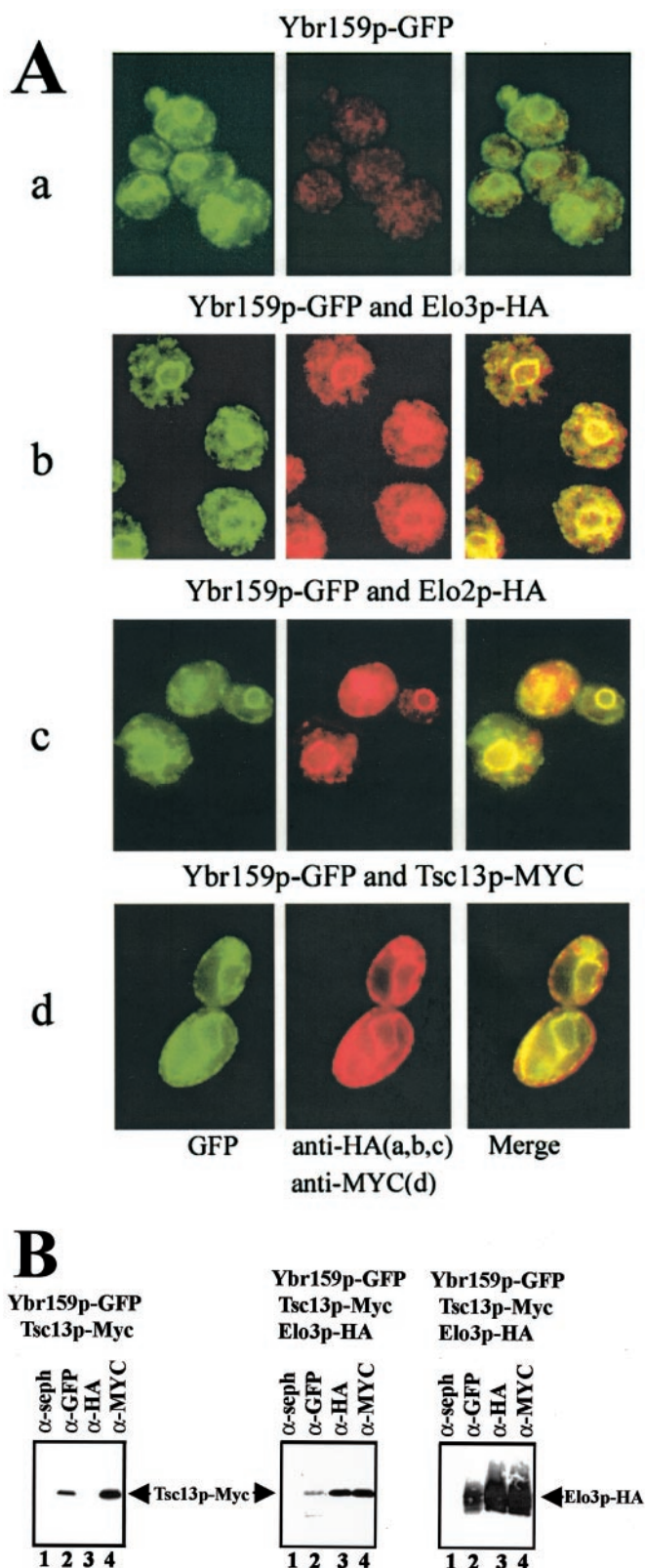
FIG. 7. **Ybr159p-GFP resides in the nuclear/ER membrane; co-localizes with Elo3p-HA, Elo2p-HA, and Tsc13p-Myc; and coimmunoprecipitates with Elo3p-HA and Tsc13p-Myc.** *A*, C-terminally tagged Ybr159p-GFP shows a typical ER localization pattern (*i.e.* around the nucleus and cell periphery). Ybr159p-GFP co-localizes with Elo3p, Elo2p, and Tsc13p. *a*, GFP fluorescence of Ybr159p-GFP; *b*, GFP fluorescence of Ybr159p-GFP and immunofluorescence of Elo3p-HA with rhodamine-conjugated anti-HA; *c*, GFP fluorescence of Ybr159p-GFP and immunofluorescence of Elo2p-HA with rhodamine-conjugated anti-HA; *d*, GFP fluorescence of Ybr159p-GFP and immunofluorescence

of Tsc13p-Myc with Cy3-conjugated anti-Myc. *B*, anti-GFP antibodies coimmunoprecipitate Elo3p-HA and Tsc13p-Myc with Ybr159p-GFP. Microsomes were prepared from cells containing Ybr159-GFP with Tsc13p-Myc alone (on *left*) or with Tsc13p-Myc and Elo3p-HA. The microsomes were solubilized, and the $100,000 \times g$ supernatant was used for immunoprecipitation with Sephadex beads (*lane 1*) or Sephadex beads conjugated to anti-GFP (*lane 2*), anti-HA (*lane 3*), or anti-Myc (*lane 4*) antibodies. The immunoprecipitated proteins were separated by SDS-PAGE and analyzed by immunoblotting with horseradish peroxidase-conjugated anti-Myc or anti-HA antibodies as indicated.

ayr1Δ single mutant indicates that it is a minor activity. This is consistent with Ybr159p being the major 3-ketoreductase of the microsomal elongase.

DISCUSSION

The main conclusion from this study is that Ybr159p is the major 3-ketoreductase activity of the endogenous yeast elongase system of enzymes required for VLCFA synthesis. This conclusion is based on several observations. The *ybr159Δ* mutant shares many of the phenotypes that are characteristic of previously studied elongase mutants, including high levels of LCBs and of medium-chain ceramides as well as low levels of VLCFAs. The *ybr159Δ* mutation is synthetically lethal in combination with an *elo2Δ* mutation, and the *ybr159Δ* mutation is a suppressor of the *csg2Δ* mutation. The *in vitro* elongation assays reveal a defect in the 3-ketoreductase activity in the mutant. These phenotypes, combined with the homology of Ybr159p to other members of the oxidoreductases, support our conclusion that this protein is a 3-ketoreductase.

Although Ybr159p is a major 3-ketoreductase responsible for VLCFA synthesis, it is not the only enzyme in yeast responsible for this activity. We provide evidence that Ayr1p is responsible for the residual 3-ketoreductase activity in the *ybr159Δ* mutant. Ayr1p was previously reported to be responsible for all of the 1-acyldihydroxyacetone-phosphate reductase activity of lipid particles as well as a significant fraction of this activity in microsomes (18). That this enzyme apparently reduces both 1-acyldihydroxyacetone phosphate and 3-keto-acyl elongation intermediates suggests that it is quite promiscuous. Whereas our data suggest that Ayr1p has 3-ketoreductase activity, it is possible that Ayr1p is essential in a *ybr159Δ* mutant for another reason. For example, its role in phosphatidic acid biosynthesis through the dihydroxyacetone pathway (18) may alter glycerophospholipid metabolism, and the combination of defects in VLCFA synthesis and glycerophospholipid metabolism may result in the synthetic lethal phenotype of the *ayr1Δ ybr159Δ* double mutant. We note, however, that deletion of the *ayr1Δ* gene in other elongase mutants (*elo2Δ* and *elo3Δ*) does not confer synthetic lethality.

In addition to reduced 3-ketoreductase activity, the *ybr159Δ* mutant is also deficient in the dehydratase activity that converts the 3-hydroxy intermediates formed during elongation to the *trans*-2,3-enoyl intermediates. The basis of the dehydratase deficiency in the *ybr159Δ* mutant is not understood, but several possibilities are suggested. For example, the Ybr159p enzyme could be bifunctional and catalyze both the 3-keto reduction and the subsequent dehydration reaction. This seems unlikely, because the protein is homologous to characterized oxidoreductases over its entire length. Another possibility is that the stability and or proper localization of the dehydratase depends on the presence of Ybr159p. There are many examples in which the loss of one component of a multienzyme complex results in the instability of other components of the complex. A third possibility is that the lack of Ybr159p, while not affecting the stability of the dehydratase, precludes formation of the elongase complex. Clearly, the condensation step is not affected by

the absence of Ybr159p, since the 3-keto intermediate is formed in the *ybr159Δ* mutant. Future studies will address whether Elo3p (and Elo2p) still associate with Tsc13p in the *ybr159Δ* mutant. Attempts to identify the putative dehydratase by co-purification with the other elongase components are also in progress.

We reported previously that the *tsc13-1* mutant, deficient in the *trans*-2,3-enoyl reductase activity of the elongase, also accumulates the 3-OH-acyl intermediate. We assumed that the lethality of the *tsc13Δ* mutant resulted from the failure to synthesize VLCFAs. The essentiality of the VLCFAs is also indicated by the synthetic lethality of the *elo2Δelo3Δ* double mutant. However, in the case of the *tsc13Δ* mutant, it remained a possibility that the lethality was actually caused by the accumulation of the 3-OH acyl intermediate. The observation that the *ybr159Δ* mutant, which accumulates high levels of the 3-OH acyl elongation intermediates, is viable (albeit slowly growing) strengthens our conclusion that the *tsc13Δ* mutant is lethal due to failure to synthesize VLCFAs.

The elongase mutants accumulate very high levels of free LCBs that do not result from reduced partitioning into ceramides. These observations indicate that either LCB synthesis is up-regulated or LCB degradation is down-regulated in the mutants. We tested whether SPT levels were elevated in the mutants and found no change in the abundance of the Lcb1p or Lcb2p proteins, or in the *in vitro* SPT activity. In the case of the elongase mutants, reduced partitioning of palmitoyl-CoA into the VLCFAs might increase flux into the LCB synthesis pathway. However, the *lag1Δlac1Δ* mutant, which is defective in acyl-CoA-dependent ceramide synthase, also displays elevated free LCBs, but this mutant also has increased levels of VLCFAs as well. That is, both LCB synthesis and VLCFA synthesis pathways appear to be up-regulated in this mutant (27, 28). Thus, it seems more likely that the synthesis of the LCBs and the VLCFAs (possibly coordinately regulated by the availability of palmitoyl-CoA in the ER) are subject to regulation by a downstream product of the sphingolipid pathway. This is most likely either ceramide or IPC, because the *csg2Δ* mutant, which is defective in mannosylation of IPC, does not accumulate LCBs or high VLCFAs.[2] Clearly, it will be important to investigate how this regulation is achieved.

The elongase mutants also synthesize medium-chain ceramides that do not arise from reversal of the Ypc1p and/or Ydc1p ceramidase activities. Thus, we propose that the medium-chain ceramides are synthesized by the acyl-CoA-dependent ceramide synthase. The accumulation of the medium-chain ceramides might simply result from reduced C26 synthesis, but again this seems unlikely because the medium-chain ceramides also accumulate in the *lac1Δlag1Δ* mutant, which synthesizes elevated levels of C26 fatty acids (27). This raises the interesting possibility that the elongase complex may associate with ceramide synthase and that the C26-acyl-CoA may be channeled from the elongase to ceramide synthase. The studies of the *lac1Δlag1Δ* mutant clearly implicate these genes in the synthesis of C26 ceramides (27, 28), but it is possible that they do not encode the ceramide synthase activity *per se*. For example, it could be (as suggested by Conzelmann and co-workers (27)) that Lag1p and Lac1p are required for conferring speci-ficity for the C26-CoA substrate to ceramide synthase. Perhaps the Lag1p/Lac1p coupling of the elongase to ceramide synthase is eliminated in either the elongase mutants or in the *lac1Δlag1Δ* mutant. This might result in loss of discrimination for C26-CoA by ceramide synthase, which would account for the medium-chain ceramides. Future experiments will be aimed at understanding the origin of the high levels of LCBs and of the medium-chain ceramides in the elongase and *lag1Δlac1Δ* mutants.

REFERENCES

1. Cinti, D. L., Cook, L., Nagi, M. N., and Suneja, S. K. (1992) *Prog. Lipid Res.* **31,** 1–51
2. James, D. W., Jr., Lim, E., Keller, J., Plooy, I., Ralston, E., and Dooner, H. K. (1995) *Plant Cell* **7,** 309–319
3. Millar, A. A., and Kunst, L. (1997) *Plant J.* **12,** 121–131
4. Roscoe, T. J., Lessire, R., Puyaubert, J., Renard, M., and Delseny, M. (2001) *FEBS Lett.* **492,** 107–111
5. Rossak, M., Smith, M., and Kunst, L. (2001) *Plant Mol. Biol.* **46,** 717–725
6. Todd, J., Post-Beittenmiller, D., and Jaworski, J. G. (1999) *Plant J.* **17,** 119–130
7. Lassner, M. W., Lardizabal, K., and Metz, J. G. (1996) *Plant Cell* **8,** 281–292
8. Dittrich, F., Zajonc, D., Huhne, K., Hoja, U., Ekici, A., Greiner, E., Klein, H., Hofmann, J., Bessoule, J. J., Sperling, P., and Schweizer, E. (1998) *Eur. J. Biochem.* **252,** 477–485
9. Toke, D. A., and Martin, C. E. (1996) *J. Biol. Chem.* **271,** 18413–18422
10. Oh, C. S., Toke, D. A., Mandala, S., and Martin, C. E. (1997) *J. Biol. Chem.* **272,** 17376–17384
11. Beaudoin, F., Gable, K., Sayanova, O., Dunn, T., and Napier, J. A. (2002) *J. Biol. Chem.* **277,** 11481–11488
12. Beaudoin, F., Michaelson, L. V., Lewis, M. J., Shewry, P. R., Sayanova, O., and Napier, J. A. (2000) *Biochem. Soc. Trans.* **28,** 661–663
13. Beaudoin, F., Michaelson, L. V., Hey, S. J., Lewis, M. J., Shewry, P. R., Sayanova, O., and Napier, J. A. (2000) *Proc. Natl. Acad. Sci. U. S. A.* **97,** 6421–6426
14. Schneiter, R., Tatzer, V., Gogg, G., Leitner, E., and Kohlwein, S. D. (2000) *J. Bacteriol.* **182,** 3655–3660
15. Beeler, T., Bacikova, D., Gable, K., Hopkins, L., Johnson, C., Slife, H., and Dunn, T. (1998) *J. Biol. Chem.* **273,** 30688–30694
16. Kohlwein, S. D., Eder, S., Oh, C. S., Martin, C. E., Gable, K., Bacikova, D., and Dunn, T. (2001) *Mol. Cell. Biol.* **21,** 109–125
17. Dunn, T. M., Gable, K., Monaghan, E., and Bacikova, D. (2000) *Methods Enzymol.* **312,** 317–330
18. Athenstaedt, K., and Daum, G. (2000) *J. Biol. Chem.* **275,** 235–240
19. Sherman, F., Fink, G. R., and Hicks, J. B. (1986) *Methods in Yeast Genetics*, Cold Spring Harbor Laboratory, Cold Spring Harbor, NY
20. Mao, C., Xu, R., Bielawska, A., Szulc, Z. M., and Obeid, L. M. (2000) *J. Biol. Chem.* **275,** 31369–31378
21. Wach, A., Brachat, A., Alberti-Segui, C., Rebischung, C., and Philippsen, P. (1997) *Yeast* **13,** 1065–1075
22. Shirra, M. K., Patton-Vogt, J., Ulrich, A., Liuta-Tehlivets, O., Kohlwein, S. D., Henry, S. A., and Arndt, K. M. (2001) *Mol. Cell. Biol.* **21,** 5710–5722
23. Haak, D., Gable, K., Beeler, T., and Dunn, T. (1997) *J. Biol. Chem.* **272,** 29704–29710
24. Gable, K., Slife, H., Bacikova, D., Monaghan, E., and Dunn, T. M. (2000) *J. Biol. Chem.* **275,** 7597–7603
25. Pringle, J. R., Adams, A. E., Drubin, D. G., and Haarer, B. K. (1991) *Methods Enzymol.* **194,** 565–602
26. Zhao, C., Beeler, T., and Dunn, T. (1994) *J. Biol. Chem.* **269,** 21480–21488
27. Guillas, I., Kirchman, P. A., Chuard, R., Pfefferli, M., Jiang, J. C., Jazwinski, S. M., and Conzelmann, A. (2001) *EMBO J.* **20,** 2655–2665
28. Schorling, S., Vallee, B., Barz, W. P., Riezman, H., and Oesterhelt, D. (2001) *Mol. Biol. Cell* **12,** 3417–3427
29. Mao, C., Ruijuan, X., Bielawska, A., and Obeid, L. (2000) *J. Biol. Chem.* **275,** 6876–6884
30. Bernert, J. T., Jr., Bourre, J. M., Baumann, N. A., and Sprecher, H. (1979) *J. Neurochem.* **32,** 85–90
31. Knoll, A., Bessoule, J. J., Sargueil, F., and Cassagne, C. (1999) *Neurochem. Int.* **34,** 255–267
32. David, D., Sundarababu, S., and Gerst, J. E. (1998) *J. Cell Biol.* **143,** 1167–1182
33. Gable, K., Han, G., Monaghan E., Bacikova, D, Natarajan, M., Williams, R., and Dunn, T. M. (2002) *J. Biol. Chem.* **277,** 10194–10200
34. Schneider, R., Brors, B., Burger, F., Camrath, S., and Weiss, H. (1997) *Curr. Genet.* **32,** 384–388

[2] K. Gable and T. M. Dunn, unpublished data.